PADEU | PADEU **15**, 21 (2005)
ISBN 963 463 557

Comparison Between Explosive Events of Two Transition Region Lines of Similar Temperatures

B. Ishak, J. G. Doyle and I. Ugarte-Urra

Armagh Observatory, College Hill, Armagh BT61 9DG, N. Ireland

E-mail: bbk@arm.ac.uk, jgd@arm.ac.uk, iuu@arm.ac.uk

Abstract
We present the difference in behavior of two transition region lines at very close temperatures, observed with SUMER/SoHO. N v 1238.82 Å shows a series of explosive events with broadenings mostly shifted to the blue. This is not seen in O v 629.73 Å, the behavior of which remains "quiet" throughout most of the time series.
Keywords: *Sun: transition region - Sun: explosive events - Sun: line profiles*

1 Introduction

It has been recognized that small-scale quiet-Sun transient events, which occur over the entire solar disk, may provide direct evidence for magnetic reconnection, plasma acceleration and heating (Harrison et al., 2003). Using space observatories, many small-scale and globally distributed solar transient events have been reported in the literature. Their potential role in fundamental processes in the solar atmosphere, such as coronal heating, mass ejection, flare activity and wind acceleration, is currently under active investigation.

One of the most discussed and studied occurrences in the literature are explosive events, the term given to transient phenomena observed at temperatures around 1×10^5 K, first discovered and classified as turbulent events and jets by Brueckner & Bartoe (1983). Explosive events are the product of magnetic reconnection (Dere et al., 1984; Porter & Dere, 1991; Innes et al., 1997; Parker, 1998; Wilhelm et al., 1998; Roussev et al., 2001). They tend to occur throughout the quiet-Sun network

where mixed-polarity magnetic features are present (Chae et al., 1998), appearing as bi-directional jets (Innes et al., 1997). Recent observations have shown a birthrate of explosive events of approximately 2500 events per second over the entire Sun, with an average size of 1800 km (Teriaca et al., 2004).

The defining characteristic of an explosive event is a highly broadened red or blue shifted spectral line, affecting either or both wings of the profile. The majority of these non-Gaussian profiles are blue-shifted with velocities up to 150 km s^{-1}. A description on explosive events identification and their general characteristics can be found in Teriaca et al. (2004).

In this work, we have analyzed a series of explosive events in the transition region lines N V 1238.82 Å and O V 629.73 Å.

2 Observation

2.1 SUMER

The Solar Ultraviolet Measurements of Emitted Radiation (SUMER) spectrograph onboard the Solar Heliospheric Observatory (SoHO) has been designed to give measurements at high spatial and spectral resolutions over wide spectral coverage that ranges from less than 500 Å to 1610 Å. Within this wavelength range, spectral imaging of the Sun at short exposure times in the Extreme Ultra Violet (EUV) emission lines permits studies of the essential physical parameters of the solar atmosphere. With SUMER, the opportunity to study and analyze the density of plasma and its temperature, abundances of species, velocity fields, topologies of the plasma structures and their evolution at high temporal resolution of a few seconds has increased tremendously.

Full discussions on the instrumentation and performance of the SUMER spectrograph are given in Wilhelm et al. (1995, 1997) and Lemaire et al. (1997).

2.2 Observational Data

The present data set was observed on 1999 June 1 from 09:13 UT to 11:01 UT with the SUMER spectrograph, pointing at Solar_X and Solar_Y coordinates of (409″,400″). In order to remain at the same location on the Sun, a rotational compensation of 0.75″ has been applied to the X-pointing throughout the observation.

The observing sequence used slit 0.3″ × 120″, exposing for 25 s on detector B. This detector has wavelength ranges of 330 Å to 750 Å for second order lines and 660 Å to 1500 Å for first order. Spectral lines of first and second orders were obtained in the observation. They were N V 1238.82 Å, N V 1242.80 Å, C I 1249 Å and Si II 1251.16 Å for the first order, and O V 629.73 Å and Mg X 624.95 Å for the second. We only consider the lines N V 1238.82 Å and O V 629.73 Å for our analysis.

Table 1 shows the summary of the observation.

Table 1: *Summary of the SUMER spectral data taken on 1999 June 1.*

Date	1999 June 1
Start Time	09:13 UT
End Time	11:01 UT
Pointing (X,Y)	(409″,400″)
Detector	B
Slit	0.3″ × 120″
Exposure Time	25 s
First Order Lines	N V 1238.82 Å, N V 1242.80 Å, C I 1249 Å, Si II 1251.16 Å
Second Order Lines	Mg X 624.95 Å, O V 629.73 Å

2.3 Data Reduction

To reduce the SUMER raw data, several steps are to be followed. In general, the standard SUMER data reduction involves decompression, reversion, dead-time correction, local gain correction, flatfield correction, geometrical distortion correction and radiometric calibration.

However, we do not go through either the decompression or reversion procedure since the Flexible Image Transport System (FITS) files used in this analysis have been decompressed and reversed onboard the space craft. Also, we do not apply the dead-time correction procedure since it is only necessary when the total counts are above 50 000 per second, which is not the case in our data set.

In order to correct for non-uniformities in the sensitivity of the detector, a flatfield correction is applied to the data set by choosing the closest date of observation for the flatfield file to be used in this process. Since we want both the rest position of the line profiles to be on the correct spectral pixel and the slit images straightened, a geometrical distortion correction is also applied to the data set. Note that the radiometric calibration, used to convert the detected intensity unit, i.e. counts per pixel per sampling interval (in our case, second) to physical units, is also not applied, leaving the data set in its original unit of counts per pixel per second.

Due to instrumental broadening, the full width at half maximum (FWHM) of the line profiles needs to be corrected by applying the *con_width_funct_3.pro* routine. All routines used in this analysis are available from the SolarSoftWare (SSW) library. We have applied the Gaussian-fitting procedure to our data set to obtain the amplitude, central position, FWHM and χ^2 of the line profiles.

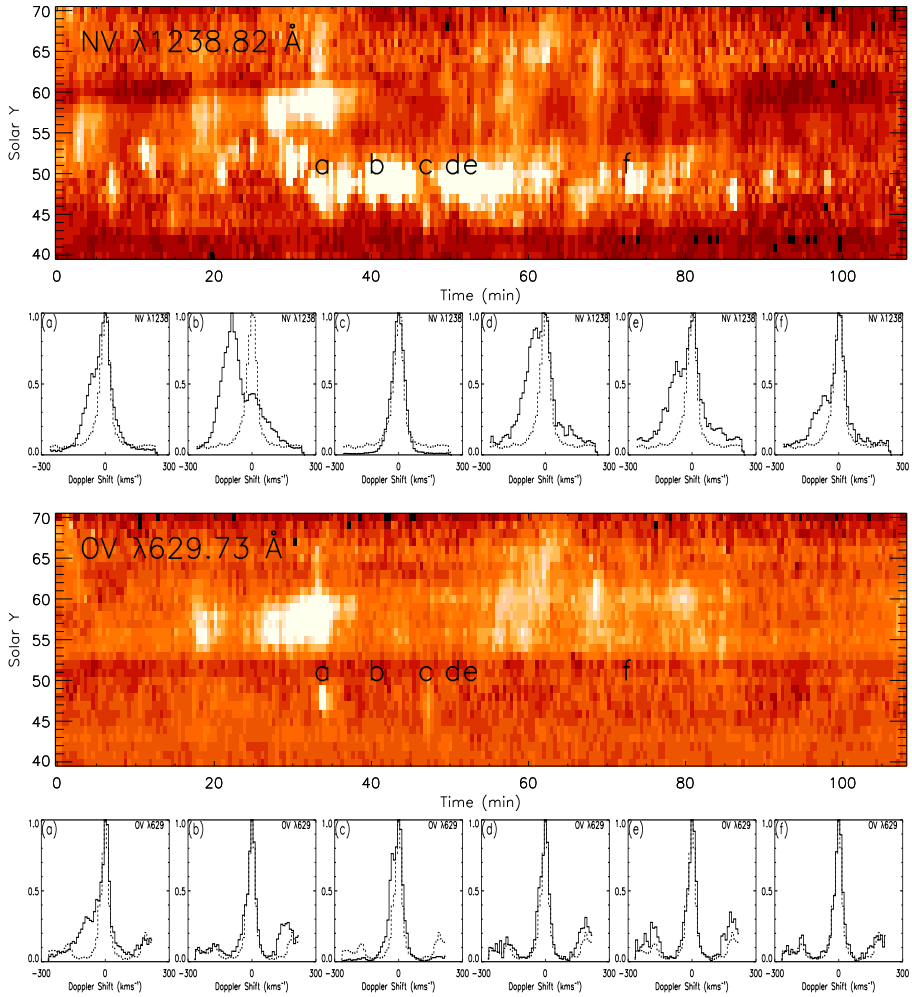

Figure 1: *Image plots of* N V *1238.82 Å and* O V *629.73 Å time series taken on 1999 June 1, starting at 09:13 UT and ending at 11:01 UT, showing the variation in the line width of a single Gaussian fit. Six different temporal locations are selected and labeled (a), (b), (c), (d), (e) and (f), corresponding to the times 09:47 UT, 09:53 UT, 10:00 UT, 10:03 UT, 10:05 UT and 10:26 UT, respectively. The selected profile plots, normalized to unity, are overplotted with the dash-lined quiet Sun profile for comparison.*

3 Results and Discussion

We have studied the two transition region lines, N v 1238.82 Å and O v 629.73 Å, and found that they behave differently so far as some explosive events are concerned, despite being formed at similar temperatures. The peak formation temperature of N v 1238.82 Å is 2×10^5 K while O v 629.73 Å is formed at 2.5×10^5 K. These temperatures are taken from CHIANTI (Dere et al., 1997; Young et al., 2003) data base, using Mazzotta et al. (1998) ionization balance calculations.

For our data analysis, we have performed a single Gaussian fitting for both N v 1238.82 Å and O v 629.73 Å to produce results in terms of amplitude, position, FWHM and χ^2 of the line profiles. χ^2 values are useful in determining the goodness of the fit.

Figure 1 shows an image plot of line width (FWHM) assuming a single Gaussian fit for each time series of N v 1238.82 Å and O v 629.73 Å. For clarity, the wider the width, the brighter it appears in both images. The "black" pixels in the images are due to bad fitting points. Plots of corresponding line profiles that have been normalized to unity for selected locations (a), (b), (c), (d), (e) and (f), at times 09:47 UT, 09:53 UT, 10:00 UT, 10:03 UT, 10:05 UT and 10:26 UT, respectively, are shown below each image. In each profile plot, the quiet Sun profile (dashed line) is overplotted for comparison.

As can be seen, except for profile (c), the line profiles of N v 1238.82 Å show prominent blue shift compared to those of O v 629.73 Å. For example, profile plot labeled (b) of N v 1238.82 Å shows an obvious shift to the blue part of the wavelength, in which a deviation from the quiet Sun profile is apparent, while the corresponding profile plot of O v 629.73 Å indicates little evidence of any such shift.

Although these two profiles are taken at the same location on the Sun and observed at the same time, the dissimilarity in their shape is conspicuous, demonstrating the absence of the explosive events phenomena in the higher temperature line, i.e. O v 629.73 Å, in this observation. The reasons for the discrepancy between the two transition region lines of N v 1238.82 Å and O v 629.73 Å are still under investigation, however, inspection at other locations show similar N v 1238.82 Å and O v 629.73 Å behavior. A possible explanation for the different behavior reported in Figure 1 may be where in the solar atmosphere these events occur.

In follow up work, we will look at the time variability of the chromospherical lines to test this idea. Furthermore, we plan to look at the formation process of the lines, in particular whether there is an effect due to electron density dependent ionization as in Doyle et al. (2005).

Acknowledgement

We wish to thank the SUMER team at Max Planck Institute for Solar System Research (MPS) (formerly Max Planck Institute for Aeronomy (MPAe)) in Lindau, Germany for their help in obtaining the data set. SUMER is part of the Solar and Heliospheric Observatory (SoHO) mission, an international collaboration between ESA and NASA.

This work was supported in part by a PRTLI research grant for Grid-enabled Computational Physics of Natural Phenomena (Cosmogrid). Research at Armagh Observatory is grant-aided by the N. Ireland Dept. of Culture, Arts and Leisure. BI would like to thank E. O'Shea for productive discussions, plus M. Madjarska and L. Xia for their help with the SUMER software.

References

Brueckner, G. E. & Bartoe, J.-D. F., 1983, ApJ, 272, 329

Chae, J., Wang, H., Lee, C., Goode, P. R., Schühle, U., 1998, ApJ, 497, L109

Dere, K. P., Bartoe, J.-D. F. & Brueckner, G. E., 1984, ApJ, 281, 870

Dere, K. P, Landi, E, Mason, H. E., Monsignori Fossi, B. C., Young, P. R., 1997, A&AS, 125, 149

Doyle, J. G., Summers, H. P. & Bryans, P., 2005, A&A, 430, L29

Harrison, R. A., Harra, L. K., Brkovic, A., Parnell, C. E., 2003, A&A, 409, 755

Innes, D. E., Inhester, B., Axford, W. I., Willhelm, K., 1997, Nature, 386, 811

Lemaire, P., Wilhelm, K., Curdt, W., Schule, U., Marsch, E., Poland, A. I., Jordan, S. D., Thomas, R. J., Hassler, D. M., Vial, J. C., Kuhne, M., Huber, M. C. E., Siegmund, O. H. W., Gabriel, A., Timothy, J. G., Grewing, M., 1997, Sol. Phys., 170, 105

Mazzotta, P., Mazzitelli, G., Colafrancesco, S., Vittorio, N., 1998, A&AS, 133, 403

Parker, E. N., 1998, ApJ, 330, 474

Porter, J. G. & Dere, K. P., 1991, ApJ, 370, 775

Roussev, I., Galsgaard, K., Erdélyi, R., Doyle, J. G., 2001, A&A, 370, 298

Teriaca, L., Banerjee, D., Falchi, A., Doyle, J. G., Madjarska, M. S., 2004, A&A, 427, 1065

Wilhelm, K., Curdt, W., Marsch, E., Schuhle, U., Lemaire, P., Gabriel, A.,Vial, J.-C., Grewing, M., Huber, M. C. E., Jordan, S. D., Poland, A. I., Thomas, R. J., Kuhne, M., Timothy, J. G., Hassler, D. M., Siegmund, O. H. W., 1995, Sol. Phys., 162, 189

Wilhelm, K., Lemaire, P., Curdt, W., Schuhle, U., Marsch, E., Poland, A. I., Jordan, S. D, Thomas, R. J., Hassler, D. M., Huber, M. C. E., Vial, J.-C., Kuhne, M., Siegmund, O. H. W., Gabriel, A., Timothy, J. G., Grewing, M., Feldman, U., Hollandt, J., Brekke, P., 1997, Sol. Phys., 170, 75

Wilhelm, K., Innes, E. E., Curdt, W., Kliem, B. , Brekke, P., 1998, ESA SP-421: Solar Jets and Coronal Plumes, 103

Young, P. R., Del Zanna, G., Landi, E., Dere, K. P., Mason, H. E., Landini, M., 2003, ApJS, 144, 135